Nonlinear Optics of Bessel Beams

T. Wulle and S. Herminghaus[a]

Fakultät für Physik, Universität Konstanz, 7750 Konstanz, Federal Republic of Germany

(Received 24 July 1992)

We investigated the frequency-doubling properties of light beams whose transverse profile is given by the zero-order Bessel function $J_0(r)$, Bessel beams. Phase-matched second-harmonic generation in a KDP crystal was observed at angles usually not suited for phase matching. It is thereby demonstrated that under certain circumstances, Bessel beams can be viewed as light beams with tunable wavelength. A variety of applications in the field of nonlinear optics is expected.

PACS numbers: 42.50.−p, 42.65.Ky, 42.79.−e

Light beams whose transverse amplitude profile is given by the zero-order Bessel function of the first kind, $J_0(r)$, have recently attracted considerable interest. Durnin discovered [1] that these beams do not exhibit any spreading although their intensity is sharply peaked near the optical axis. Since at first glance this seems to contradict the uncertainty principle, the term "diffraction-free beam" was coined and is commonly used. However, in what follows we prefer the more technical (and more adequate) term "Bessel beam."

Since the first experimental realization of a Bessel beam [2], many potential applications have been pointed out [3,4], all utilizing the mentioned absence of spreading. In contrast, no significant attention has been given to the fact that the propagation constant of a Bessel beam $\beta=(k^2-\alpha^2)^{1/2}$ differs from the wave number $k=2\pi/\lambda$ of a plane wave. In other words, the "wavelength" of a Bessel beam, measured along the optical axis where the intensity is high, differs from that of a usual (e.g., Gaussian) beam of the same frequency. In this paper, we want to demonstrate the consequences of this feature for the interaction of a Bessel beam with an optically nonlinear medium.

The first Bessel beams produced experimentally were of rather low intensity, whereas the investigation of nonlinear optical effects requires high-intensity pump beams. Turunen, Vasara, and Friberg [5] introduced a type of zone plate which converts a large fraction of the light by which it is illuminated into a Bessel beam. It consists of an array of concentric circles, reminiscent of a Fresnel zone plate, but with constant radius increment from one circle to the next. Thus, it can be viewed as a circular diffraction grating which yields, at first-order diffraction, a cone of plane waves when illuminated with parallel light. The interference pattern appearing within this cone is the desired Bessel beam [1]. Its field distribution can be calculated from Kirchoff's diffraction theory [6] which yields, in scalar field approximation,

$$E(r,z)=J_0(\alpha r)e^{-i(k^2-\alpha^2)^{1/2}z}\sqrt{z} \qquad (1)$$

(r is the distance from z, the coordinate along the optical axis). The diameter of the beam as well as its propagation constant is determined by the parameter α, which depends only on the radius increment g of the circles on the zone plate and is given by $\alpha=2\pi/g$. For our experiments, a computer-generated array of 300 concentric circles was printed on a high-resolution laser printer (2500 dpi), and was then photographically reduced. The zone plate obtained in this way had a diameter of approximately 1 cm and a radius increment of $g=17.5$ μm.

By illuminating this zone plate with parallel light from a Q-switched Nd:YAG laser ($\lambda=1064$ nm; pulse energy ≈ 1 mJ), a Bessel beam was produced and subsequently imaged as indicated in Fig. 1. The lens L and the zoom lens Z are positioned so as to make their focal planes coincide. Consequently, a plane wave entering L will emerge from the zoom lens as a plane wave. The cone of plane waves generated by the zone plate is thus transformed into another cone of plane waves behind the zoom, with the important property that the cone angle can be continuously varied by varying the focal length of the zoom. Hence, the Bessel beam generated by the zone plate is transformed by the combination of L and the zoom into another Bessel beam whose propagation constant β can be varied continuously according to

$$\beta=k[1-(\alpha f_L/kf_Z)^2]^{1/2}, \qquad (2)$$

where f_L and f_Z are the focal lengths of the lens L and the zoom lens Z, respectively.

Let us now consider what we expect for the frequency-

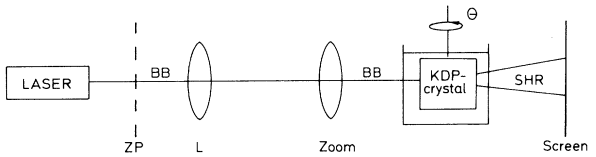

FIG. 1. Schematic of the experimental setup. ZP: zone plate, illuminated by the expanded laser beam (Q-switched Nd:YAG; approximately 1 mJ per pulse). BB: Bessel beam. L: lens. Zoom: zoom lens whose focal plane coincides with the focal plane of the lens L. SHR: second-harmonic radiation. The KDP crystal (length 15 mm) can be rotated in a fixed cuvette containing index-matching fluid. Distortions of the Bessel beam by refraction from the tilted crystal surfaces are thus prevented.

doubling behavior of the Bessel beam in an optically nonlinear material. Since second-harmonic generation (SHG) is a two-photon process, the wave vector of a second-harmonic photon is the vector sum of the wave vectors of two incoming photons, by momentum conservation. As mentioned, the Bessel beam can be viewed as a superposition of infinitely many plane waves whose wave vectors lie on a cone in k space. Obviously, all pairs of photons with mutually opposite radial components of their wave vectors contribute to SHG *on the optical axis*, with a wave number equal to 2β. Consequently, in addition to a cone of second-harmonic polarization from the individual plane waves, we expect as strong second-harmonic polarization wave traveling in the z direction, with a wave number differing from the usual value of $2k$. Furthermore, since the intensity of the second-harmonic polarization is sharply peaked on the optical axis, the Bessel beam behaves as a well-collimated light beam with anomalous wave number.

At this point, we should mention the relationship between our experiment and the recently developed technique of noncollinear SHG [7], where two pump beams are superposed at some angle on which the phase-matching conditions depend. The important difference is that in our case, SHG takes place effectively only close to the optical axis where the intensity has its maximum. The peculiar nonlinear optical properties of Bessel beams are a consequence of the combination of the anomalous on-axis wave number and the specific spatial intensity distribution.

As is well known, effective SHG is possible only when the phase velocities of the fundamental and the frequency-doubled radiation coincide, i.e., at the intersection of the indicatrixes of the fundamental and the frequency-doubled radiation [8]. In a suitable crystal (KDP in our case), such an intersection exists at a particular angle θ_{PM}^{0} (with respect to the crystal axes), the so-called phase-matching angle. Since the wave number of the on-axis second-harmonic polarization due to the Bessel beam differs from that of a Gaussian beam, so does its phase velocity, and we expect to observe phase matching at an angle θ_{PM} different from the usual phase-matching angle θ_{PM}^{0}. Furthermore, since we are able to tune the propagation constant continuously, phase matching at a variety of angles (depending on tuning) should be possible.

That this is indeed so is shown in Fig. 2 where the second-harmonic intensity measured on the optical axis behind the crystal is plotted as a function of the angular position θ of the crystal. Two intensity peaks are present. The one on the right corresponds to SHG from the Bessel beam; the one on the left (at $\theta=\theta_{PM}^{0}$) indicates SHG from the parallel light transmitted through the zone plate without being diffracted. The position of the right peak depends on the focal length of the zoom lens and thus on the propagation constant β of the Bessel beam, thus demonstrating the tunability of the phase-matching angle. The range of tuning is limited essentially by the type of zoom lens used in our experiment.

Figure 3 shows a plot of the quantity $\Delta:=(k-\beta)/k$, which can be calculated from Eq. (2), as a function of the angle θ_{PM} of the KDP crystal at which phase-matched SHG from the Bessel beam occurs. At phase matching, Δ is proportional to the difference of the refractive indices for the fundamental and the frequency-doubled light. Therefore, the data in Fig. 3 give a "topography" of the birefringence in the vicinity of the standard phase-matching angle. The straight line represents a least-squares fit to the data and has a slope of $(6.6\pm0.6)\times10^{-4}$ deg^{-1}. For comparison, the change in birefringence near the phase-matching angle can be in-

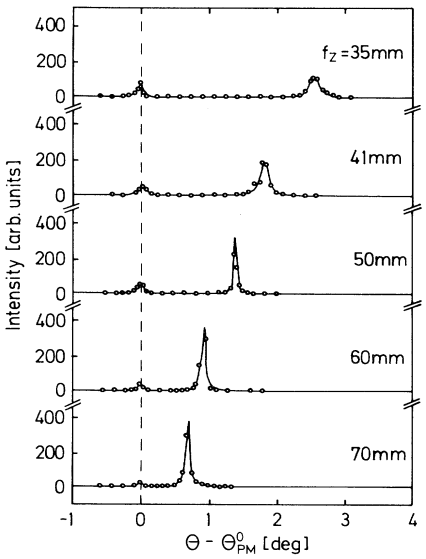

FIG. 2. SHG intensity as a function of detuning from the standard phase-matching angle θ_{PM}^{0}, for different focal lengths f_Z of the zoom lens. The solid lines serve as guides to the eye.

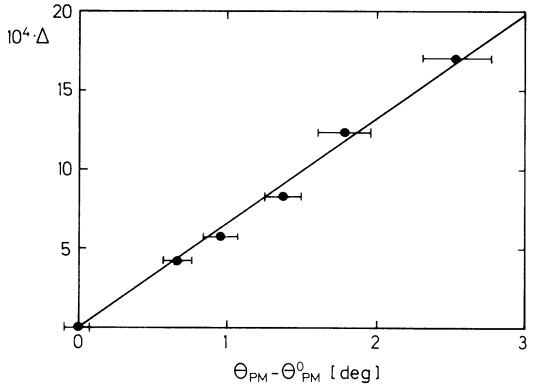

FIG. 3. The quantity $\Delta:=(k-\beta)/k$ at which phase matching occurs as a function of the angular position of the crystal. The error bars indicate the width of the peaks in Fig. 2. The slope of the straight line is $(6.6\pm0.6)\times10^{-4}$ deg^{-1}.

ferred from the ordinary and extraordinary refractive index of the crystal [8]. One obtains $(5.9 \pm 0.5) \times 10^{-4}$ deg^{-1}, in agreement with the measured value.

The demonstrated tunability of the wave number has several potential applications in the field of nonlinear optics, wherever phase-matching problems are encountered. For instance, in new optically nonlinear materials the usual phase-matching parameters (temperature and angle of incidence) are not always suitable, so novel tuning parameters are desirable. Furthermore, it becomes possible to perform parametric down-conversion in materials which usually are not phase matchable at all [8]. Very promising among these are, e.g., GaAs and methyl-nitroaniline which have a nonlinearity several orders of magnitude larger than that of $LiNbO_3$ [9,10]. In stimulated Raman scattering experiments, phase matching of the molecular polarization wave to the infrared radiation should be achievable, yielding a novel source of intense infrared radiation. We are currently performing experiments which investigate these possibilities.

We now want to discuss the far-field intensity distribution of the frequency-doubled radiation. Its transverse profile is given by the Fourier transform of the SHG polarization in the crystal, $P^{(2)}(\mathbf{r})$. With

$$E(r,z) \propto J_0(\alpha r) e^{-i(k^2-\alpha^2)^{1/2}z} \tag{3}$$

and $P^{(2)} = \chi^{(2)} E^2$ we obtain, in k space,

$$P^{(2)}(k_r,k_z) \propto \chi^{(2)} F\{J_0^2(\alpha r)\} \delta(k_z - 2\beta), \tag{4}$$

where $F\{\cdots\}$ denotes the two-dimensional Fourier transform and $\delta(\cdots)$ is Dirac's δ function. Phase matching will occur when there is an overlap of $P^{(2)}$ with the indicatrix of the frequency-doubled radiation. The δ function tells us that phase matching is possible only on the intersection of this indicatrix with the plane defined by $k_z = 2\beta$. The set of k vectors belonging to such an intersection forms a cone which we will call the Cherenkov cone, in accordance with other papers in this field [11,12]. The Fourier transform of $J_0^2(\alpha r)$ is readily shown to be given by

$$F\{J_0^2(\alpha r)\} = \frac{2}{|k_r|(4\alpha^2 - k_r^2)^{1/2}} \tag{5}$$

and will be called the efficiency function from now on. Efficient SHG will occur when the Cherenkov cone intersects one of the poles of the efficiency function. The strong pole at $|k_r| = 0$ corresponds to SHG along the optical axis with a wave number 2β, which is characteristic of the Bessel beam. The weaker poles along the circle $|k_r| = 2\alpha$ correspond to SHG from the individual plane waves in the cone.

Figure 4 shows photographs of the far-field intensity distribution for $\theta \neq \theta_{PM}$ [Fig. 4(a)] and for $\theta = \theta_{PM}$ [Fig. 4(b)]. In Fig. 4(c), the locus of the poles of $F\{J_0^2(\alpha r)\}$ is plotted to the same scale. The dashed circles (a) and (b) indicate the Cherenkov cones which are visible as faint

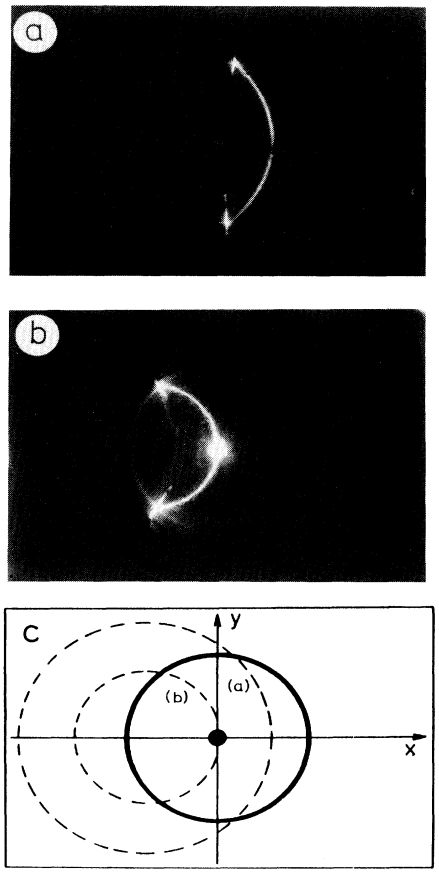

FIG. 4. Far-field intensity distribution of the second-harmonic radiation. (a) No phase matching; part of the Cherenkov cone is visible as a circle segment. (b) Phase matching; the Cherenkov cone intersects the optical axis. (c) Plot of the locus of the poles of the efficiency function (solid line and central spot). The strongest pole lies on the optical axis. The dashed circles indicate the Cherenkov cones from (a) and (b).

circles in Figs. 4(a) and 4(b), respectively. A plot of several Cherenkov cones for different tuning parameters would yield a contour map of the indicatrix of the frequency-doubled light.

The bright spot in the center of Fig. 4(b) demonstrates efficient SHG of the Bessel beam in the direction of the optical axis. It occurs when the Cherenkov cone meets the central pole of the efficiency function. The divergence of this central beam is approximately 1 mrad. Note that the photograph does not correctly account for the large difference in intensities of the on-axis and the off-axis SHG. While on-axis SHG could be easily measured (cf. Fig. 2), the intensity of the Cherenkov cone was below our limits of detection.

When the propagation constant β of the Bessel beam and the crystal angle θ are not in accordance for phase matching, as in Fig. 4(a), the Cherenkov cone misses the central pole and efficient SHG does not occur. Intersec-

tions with the pole at $|k_r| = 2\alpha$ correspond to SHG from the individual plane waves and can be clearly seen as intensity maxima, as in Fig. 4(b). At these points, however, conversion is comparably weak since this pole is not as strong as the one at $|k_r| = 0$.

In conclusion, demonstrating the tunability of the phase-matching condition for SHG from a Bessel beam, our experiments show that under certain circumstances, Bessel beams can be viewed as light beams with tunable wavelength. This result is not only interesting from a fundamental point of view; wherever phase-matching problems are encountered in the nonlinear interaction of two light waves of different frequency (i.e., almost everywhere in the field of nonlinear optics), the Bessel beam offers an additional tuning parameter.

We thank Paul Leiderer for many pleasant and inspiring discussions and for making available to us the facilities of his research group. We are indebted to Bob Riekert from T. J. Watson Research Center (IBM) for his help with the production of the zone plate.

[a]To whom correspondence should be addressed.

[1] J. Durnin, J. Opt. Soc. Am. A **4**, 651 (1987).
[2] J. Durnin, J. J. Miceli, and J. H. Eberly, Phys. Rev. Lett. **58**, 1499 (1987).
[3] G. Häusler and W. Heckel, Appl. Opt. **27**, 5165 (1988).
[4] J. Lu and J. F. Greenleaf, IEEE Trans. Ultrason., Ferroelectrics, and Freq. Control **39**, 19 (1992), and references therein.
[5] J. Turunen, A. Vasara, and A. T. Friberg, Appl. Opt. **27**, 3959 (1988).
[6] A. Vasara, J. Turunen, and A. T. Friberg, J. Opt. Soc. Am. **6**, 1748 (1989).
[7] A. Reichert and K. Betzeler, "Characterization of Electro-optic Crystals by Non-Collinear Frequency Doubling" (to be published).
[8] This process can be understood as the inverse of so-called Cherenkov SHG; see Ref. [11].
[9] F. Zernike and J. E. Midwinter, *Applied Nonlinear Optics* (Wiley, New York, 1973).
[10] M. Kiguchi, M. Kato, M. Okunaka, and Y. Taniguchi, Appl. Phys. Lett. **60**, 1933 (1992).
[11] A. Zembrod, H. Puell, and J. A. Gjordmaine, Optoelectron. Lett. **1**, 64 (1969).
[12] P. K. Tien, R. Ulrich, and R. J. Martin, Appl. Phys. Lett. **17**, 447 (1970).

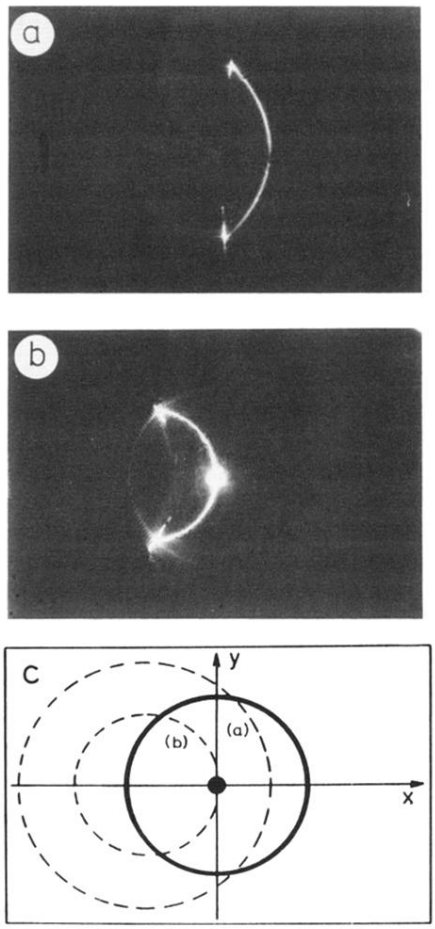

FIG. 4. Far-field intensity distribution of the second-harmonic radiation. (a) No phase matching; part of the Cherenkov cone is visible as a circle segment. (b) Phase matching; the Cherenkov cone intersects the optical axis. (c) Plot of the locus of the poles of the efficiency function (solid line and central spot). The strongest pole lies on the optical axis. The dashed circles indicate the Cherenkov cones from (a) and (b).